

The recognition of blazars and the blazar spectral sequence

S. Antón^{1,2} *, I.W.A. Browne¹

¹ *Jodrell Bank Observatory, University of Manchester, Macclesfield, Cheshire, SK11 9DL, U.K.*

² *CAAUL, Observatório Astronómico de Lisboa, Tapada de Ajuda, 1349-018, Lisboa, Portugal.*

ABSTRACT

We analyse a group of radio sources, a subset of the 200 mJy sample, all of which have core-jet radio structures measured with VLBI and have flat spectra stretching from the radio to the millimetre/sub-millimetre band. Thus the objects have most of the properties expected of blazars. However, they display varied optical properties ranging from “Seyfert-like” objects, through BL Lac objects, to “normal” elliptical galaxies. We investigate the distribution of synchrotron peak frequencies in their Spectral Energy Distributions (SEDs) and find a broad distribution between 10^{12} and 10^{16} Hz. Our conclusion is that we should consider virtually all objects in the sample as blazars since much of the diversity in their classification based on traditional optical criteria arises from differences in the frequency at which the non-thermal emission begins to decline. Specifically, an object is only classified as BL Lac when its peak frequency falls in the near IR/optical range. We determine peak frequencies using the same method for objects from other blazar samples. An important result is that our objects do not follow the blazar spectral sequence proposed by Fossati et al. and Ghisellini et al. in which, on average, peak frequencies increase as the radio luminosity decreases. Most of our low radio-luminosity sources have peaks in their SEDs at low frequencies, not at the expected high frequencies. We suggest that at least part of the systematic trend seen by Fossati et al. and Ghisellini et al. results from selection effects.

Key words: galaxies: active - BL Lacertae objects: general.

1 INTRODUCTION

Blazars are radio sources that have prominent synchrotron cores. Their broad-band spectra are smooth and flat from the radio up to the infrared/optical bands (or beyond that), the emission is variable, sometimes on time-scales as short as minutes to hours, and is often polarised (see e.g. Urry & Padovani (1995) and Kollgaard (1994) for reviews). The blazar population comprises BL Lacs and Flat Spectrum Radio Quasars, which are, respectively, featureless optical spectrum objects and strong broad emission line objects. It is believed that the continuum radiation of blazars is predominantly non-thermal emission from a relativistic jet pointing to the observer at a small angle to the line of sight, as proposed by Blandford & Rees (1978). Traditionally, apart from the radio-loudness, core-jet morphology and flatness of the broad-band spectrum, an object is only classified as a BL Lac if it has a strong non-thermal optical component relative to the starlight and weak emission lines. The emission lines are commonly quantified by the equivalent width (EW) of the brightest line and the strength of the non-thermal optical component is measured

through the relative depression of the continuum at 4000 \AA , the 4000 \AA break contrast, C . The usual limits adopted are $EW < 5 \text{ \AA}$ and $C < 0.25$ (e.g. Stocke et al., 1991). These are empirical limits, based on the properties of a relatively small number of objects. Results from newer samples have been showing that the 4000 \AA break contrast distribution of BL Lacs and other “non-BL Lac” objects does not reveal a clear bi-modality (e.g. Marchã et al., 1996; hereinafter M96, Laurent-Muehleisen et al., 1998; Caccianiga et al., 1999; Rector et al., 2000). As first noted by M96 the traditional classification of a BL Lac is almost certainly too restrictive, and an “expanded” definition that includes objects with $C < 0.4$ and objects with larger emission line equivalent widths was proposed. More recently, Landt et al. (2004) have suggested that there is a natural separation between weak- and strong-lined sources in the $[\text{OIII}] 5007 \text{ \AA}/[\text{OII}] 3727 \text{ \AA}$ plane which clarifies blazar classification schemes. Their weak-lined class contains the majority of classical BL Lacs while the strong-lined class has the majority of the broad-line blazars. Their approach is interesting but might be complicated by the fact that they include a wide range of luminosities in their sample. In this paper we look at continuum spectral energy distributions (SED)

* e-mail: Sonia.Anton@oal.ul.pt

of objects in a sample with a restricted range of luminosities.

The SEDs of blazars are distinctive by having a 2-hump shape, in units of νF_ν vs. ν (F_ν the flux density and ν the frequency). In general, the lower frequency hump is attributed to synchrotron radiation and the second hump to inverse Compton scattering by the synchrotron electrons. The first hump is characterised by the frequency ν_{peak} at which the synchrotron component begins to decline. This frequency is directly related to a break in the synchrotron electron energy spectrum in the jet. Some BL Lacs (and Flat Spectrum Radio Quasars) show the first energy peak in the infrared/optical wavelength range and these are often labelled Low frequency peaked BL Lacs (LBLs). On the other hand there are those that show the first energy peak in the EUV region, the high frequency peaked BL Lacs (HBLs). LBLs are mainly found in the radio-selected samples, whereas the HBLs are mainly found in the X-ray selected samples. Although some authors disagreed (e.g. Polatidis, 1989), for some time it was thought that there was a bi-modal LBL-HBL population. However, the discovery of more BL Lacs, mainly in the X-ray/radio surveys, has been showing that there is a continuous distribution of the peak frequencies (e.g. Perlman et al. 1998, 2001) and that the apparent dichotomy was due to selection effects (e.g. Padovani et al. (2003) and references therein). It is now widely accepted that BL Lacs have a broad ν_{peak} distribution, spanning ~ 5 orders of magnitude in frequency ($10^{13} < \nu_{peak} < 10^{18}$ Hz), the extremes being populated by LBLs and HBLs.

A potentially very important result has been pointed out by Fossati et al. (1998) and Ghisellini et al. (1998, 2002). They found a sequence involving the frequency at which the peak of the non-thermal emission occurs and the radio luminosity; the synchrotron peak position and the radio luminosity appear anti-correlated in the sense that lower peak positions are associated with the more luminous radio emitters. Donato et al. (2001), based on X-ray spectra of blazars, also found the same anti-correlation. This recognition of a blazar spectral sequence appears to be an important breakthrough in our understanding and it is therefore vital to check if the result holds when a wider range of parameter space is explored.

Much of the research on blazars has been based on very bright and relatively small samples, either selected on the radio band, e.g. “1 Jy sample” (Stickel et al., 1991) or in the X-ray band, e.g. EMSS¹ (Gioia et al., 1990; Stocke et al., 1991; Maccacaro et al., 1994). As a consequence, the knowledge on these objects has been built on the properties of the most powerful ones, which may not be representative of the population as a whole. It would be, therefore, very useful to have a new radio-selected sample of relatively low radio-luminosity objects in order to investigate further the luminosity-peak frequency sequence. In particular, if the trend in the data is telling us about the physical properties of the blazars, and not about selection effects, the low-luminosity objects should be found to have relatively high

synchrotron peak frequencies. Such an investigation is particularly timely as recent results point to a more complicated scenario, in which objects from deep surveys do not follow the anti-correlation trend (Padovani et al., 2003).

In order to investigate this issue and others we have been analysing a low-luminosity radio-selected sample, the 200 mJy sample (Antón et al, 2004, hereinafter A04; M96). Producing statistically well-defined samples of blazars is difficult since traditionally it has relied on the detection of an optical non-thermal component in the SED. This introduces strong luminosity-dependent selection effects (Browne & Marchã, 1993; Marchã & Browne, 1995, Landt et al. 2002, 2004; Rector & Stocke, 2001) and many analyses of blazar population statistics can be suspect for this reason. Therefore we have been exploring an approach to sample selection focusing on the low frequency (radio, mm and sub-mm) properties, particularly the possession of milliarcsecond VLBI core-jet structure of the type commonly found in superluminal radio sources. With our 200 mJy core-jet sample we have a set of objects well suited to extend our knowledge of the SEDs of blazar-like objects. Here we address the following questions:

- What is the range of synchrotron peak frequencies amongst the low-luminosity radio selected objects? Do these objects follow the luminosity peak frequency sequence?
- How does the peak frequency influence the classification of the objects?
- Are there any selection effects influencing the luminosity peak frequency sequence?

The paper is organised as follows. In section 2 we present a summary of the properties of the sources discussed here, as well as the analysis of their SEDs. In section 3 we discuss the relation between the SED type and the optical classification of the objects. The properties of the 200 mJy objects in the framework of the spectral sequence found by Fossati et al. (1998) and Ghisellini et al. (1998, 2002) are analysed in section 4. Specifically, we fit a model consisting of a low frequency power law plus a higher frequency parabola to both the 200 mJy SEDs and those from other samples in order to look for systematic trends. The main points of this work are summarised in section 5. Throughout the paper we assume $H_0 = 65 \text{ kms}^{-1} \text{ Mpc}^{-1}$ and $q_o=0$.

2 THE SEDS

2.1 The sample of objects

The objects analysed in this paper are a subsample of the 200 mJy sample (A04, M96). This is a nearby radio-selected sample (most of the objects have $z < 0.2$), that comprises objects with core-dominated morphology at 8.4 GHz, with $S_{5\text{GHz}} \geq 200$ mJy, flat radio spectra between 1.4 and 5 GHz ($\alpha_{1.4}^{5.0} \geq -0.5$) and $R \leq 17$ mag.

The objects under consideration in the present work are presented in Table 1. They were selected on the basis of the results from the multiwavelength study of the 200 mJy sample, presented in A04. That study has revealed a subset of objects with uniform radio/mm properties, flat broadband spectra, some being classified as BL Lac objects but some having different optical classifications, as follows:

¹ Einstein Extended Medium Sensitivity Survey

Object B1950	Radio morph.	z	Optical class	SED type	T_B $\times 10^9$ K
0055+300	c+j ¹⁴	0.015	PEG	BPL+IB	6.2 ^{1,a}
0109+224	c+j ¹³		BLL	BPL	12.2 ^{2,b}
0125+487	c+j ¹	0.067	Sy1	BPL	1.5 ^{2,b}
0149+710	c+j ¹	0.022	PEG	BPL+IB	2.4 ^{2,b}
0210+515	c+j ¹	0.049	BLL	BPL	0.8 ^{2,b}
0251+393	c+j ⁷	0.289	Sy1	BPL	15.0 ^{3,b}
0309+411	c+j ⁷	0.134	Sy1	BPL	
0321+340	c+j ⁹	0.061	Sy1	BPL	
0651+428	c+j ¹	0.129	BLC	BPL	1.0 ^{2,b}
0716+714	c+j ³		BLL	BPL	4.6 ^{1,a}
0806+350	c+j ²	0.082	BLL	BPL	0.8 ^{2,b}
0912+297	c+j ¹³		BLL	BPL	
1055+567	c+j ¹	0.144	BLL	BPL	2.4 ^{2,b}
1101+384	c+j ¹¹	0.031	BLL	BPL	7.8 ^{1,a}
1123+203	c+j ⁹	0.133	BLL	BPL	
1133+704	c+j ⁸	0.046	BLL	BPL	
1144+352	c+j ⁷	0.063	PEG	BPL+IB	
1147+245	c+j ⁴		BLL	BPL	
1215+303	c+j ¹	0.130	BLL	BPL	4.2 ^{2,b}
1219+285	c+j ⁵	0.102	BLL	BPL	3.2 ^{1,a}
1241+735	c+j ¹	0.075	PEG	BPL	1.8 ^{2,b}
1246+586	c+j ¹²		BLL	BPL	8.0 ^{4,b}
1418+546	c+j ⁴	0.151	BLL	BPL	
1421+511	c+j ⁹	0.274	Sy1	BPL	
1424+240	c+j ⁹		BLL	BPL	
1551+239		0.117	PEG	BPL+IB	
1646+499	c+j ¹	0.049	Sy1	BPL	1.4 ^{2,b}
1652+398	c+j ¹⁰	0.030	BLL	BPL	6.7 ^{1,a}
1658+302		0.036	PEG	BPL+IB	
1744+260	c+j ¹⁵	0.147	Sy2	BPL	
1807+698	c+j ⁶	0.051	BLL	BPL	13.2 ^{1,a}
1959+650	c+j ¹	0.047	BLL	BPL	2.4 ^{2,b}
2116+81	c+j ¹⁶	0.084	Sy1	BPL	
2320+203	c+j ²	0.038	PEG	BPL	0.8 ^{2,b}

Table 1. 1st column 1950.0 IAU name of the object, 2nd column is the radio morphology, 3rd column is the optical classification, 4th column is the SED type, 5th column is the brightness temperature. *Radio morphology classification key:* (c+j) core+jet VLBA structure according to: 1. Bondi et al. (2001) 2. Bondi et al. (2004) 3. Gabuzda et al. (1998) 4. Gabuzda et al. (1996) 5. Gabuzda & Cawthorne (1996) 6. Gabuzda et al. (1989) 7. Henstock et al. (1995) 8. Kollgaard et al. (1996) 9. NRAO VLBA calibrators list 10. Pearson et al. (1993) 11. Piner et al. (1999) 12. Taylor et al. (1994) 13. USNO Astrometric VLBI database 14. Venturi et al. (1993) 15. The object 1744+260 shows core-jet morphology at MERLIN resolution (Augusto et al., 1998). 16. Taylor et al. (1996). *Optical classification keys:* **BLL**=BL Lac, **BLC**=BL Lac Candidate, **Syf1**=Seyfert-1 type, **Syf2**=Seyfert-2 type, **PEG**=Passive Elliptical Galaxies. *SED classification keys:* **BPL+IB** broadband flat spectra with one or more bumps, **BPL** broken power-law broadband spectra. The brightness temperatures were computed from VLBI maps, at ^a 15 GHz or ^b 5 GHz presented in: 1. Kellermann et al. (1998) 2. Bondi et al. (2004) 3. Henstock et al. (1995) 4. Taylor et al. (1994)

(i) From the analysis of the SEDs of the 200 mJy sample as a whole (A04), it became clear that there was a subset of objects which had, at least at wavelengths down to the sub-mm, flat broadband spectra (in units of flux density vs frequency) before steepening, and they have been classified as broken-power-law type objects (**BPL**) in Table 1. There are a few objects showing an infrared bump that we inter-

preted as dust emission, and they are listed in Table 1 as **BPL+IB** (broken-power-law + infrared bump)².

(ii) All the objects have a **core-jet** radio structure when observed with VLBI techniques (Bondi et al 2004, 2001 and references in Table 1). This ensures that we are dealing with a set of objects in which the radio emission is mainly from the active nucleus and not from compact lobes, as would be the case with sources with CSO-like radio structures. In addition we note that the possession of core-jet VLBI radio structures is in general a good circumstantial evidence that we are dealing with emission from relativistic jets. For example, Britzen et al. (Britzen, personal communication) have made extensive VLBI observations of a complete sample of 297 flat spectrum radio sources (CJF: Taylor et al. 1996) and they find that $\sim 90\%$ of those CJF sources with core jet structures show superluminal motion.

For most of the objects the brightness temperatures could be estimated, and they are presented in Table 1. The temperatures were computed according to:

$$T_B = 1.8 \times 10^9 \frac{S_\nu [\text{mJy}]}{\nu^2 [\text{GHz}] \Theta^2}$$

with Θ being the source size in milliarcsec (Caccianiga et al., 2001). Note that T_B is a lower limit, as the size of the emitting region is most probably smaller than the beamsize. All the objects have brightness temperatures larger than 10^8 K, showing that the emission is certainly non-thermal in origin. More interesting is the fact that the T_B of BL Lacs and of the other objects are very similar.

(iii) Based on optical spectral properties of the objects, in particular the 4000 Å break contrast and emission line strength, they are classified as (see A04 and M96):

- BL Lac objects (**BLL**), objects that obey the “classical” BL Lac definition: $C \leq 0.25$ and $EW \leq 5$ Å.
- BL Lac Candidates (**BLC**), objects with relatively small break contrast and $EW: 0.25 < C < 0.4$ and $EW < 40$ Å.
- Seyfert-like objects, objects with relatively strong broad (**Sy1**) or narrow (**Sy2**) emission lines: $EW > 40$ Å.
- Passive Elliptical Galaxies (**PEGs**), objects with high contrast and weak emission lines: $C \geq 0.40$ and $EW < 40$ Å.

2.2 Fitting the SEDs

The multiwavelength study of the 200 mJy sample has revealed an homogeneous subset of objects which have many of the properties expected of BL Lacs but not all of which met the traditional BL Lac selection criteria. As it can be inferred from Table 1 all the objects that are optically classified as BL Lacs have SEDs which fall into the category BPL. More interesting is the fact that objects other than BL Lacs look similar to BL Lacs up to relatively high frequencies. To investigate this further, the SEDs of the objects in Table 1 were model fitted to estimate the peak frequency, and look for any statistical difference between BL Lacs and non-BL Lac objects. We assumed the Fossati et al. (1997) model, that consists of a power-law, to represent the low frequencies, plus a parabola for the higher frequencies. The model differentiates two frequencies: up to a certain frequency the radiation is taken to be optically thick and it is

² see A04 for details; there the BPL+IB and the BPL are called type II and III respectively.

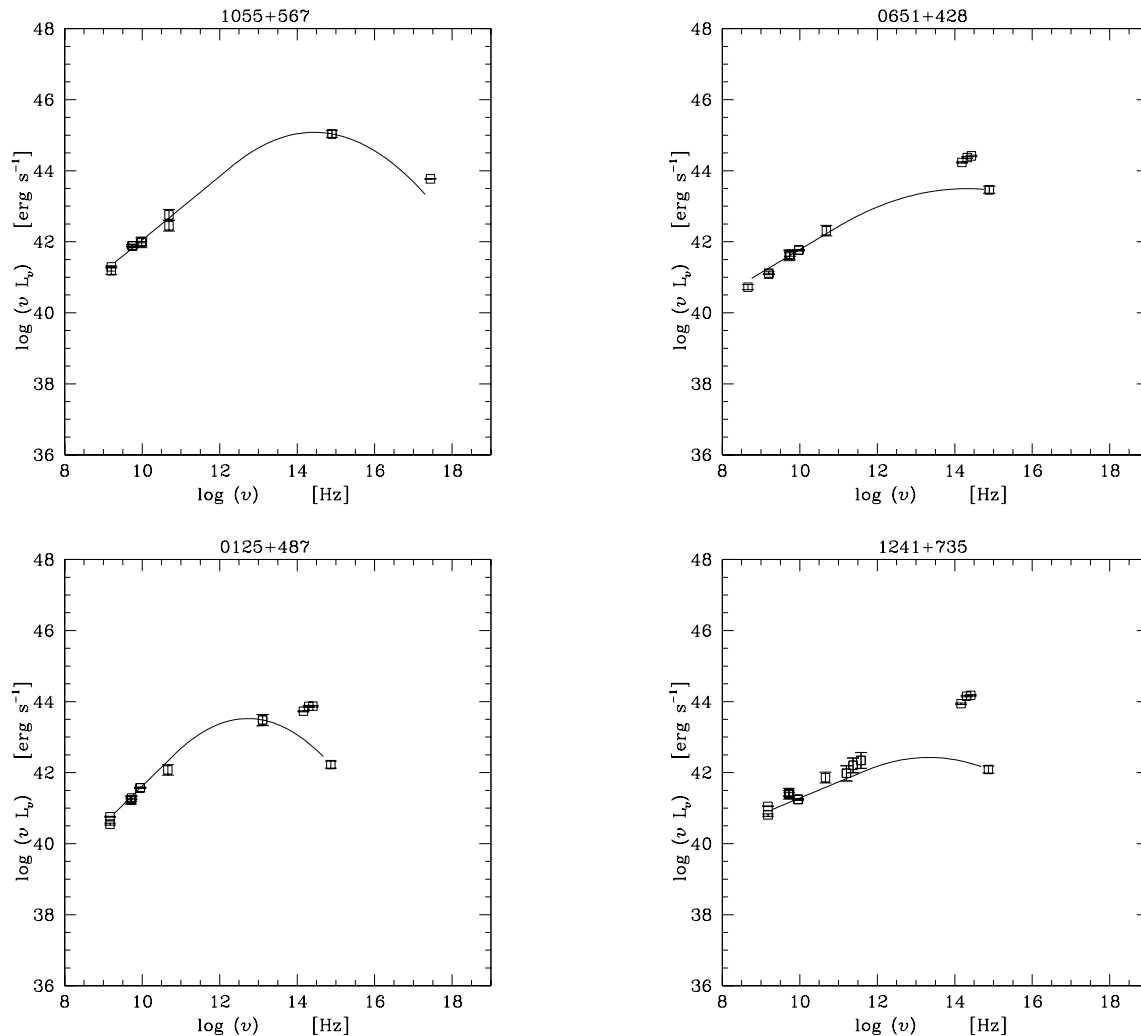


Figure 1. Spectral energy distributions, in units of $\log(\nu L_\nu)$ vs $\log(\nu)$, of objects with different optical classification: BL Lac object 1055+567, BL Lac Candidate object 0651+428, Seyfert-1 like object 0125+487 and the PEG 1241+735. The data are from A04. The superimposed line is the fit of a power-law together with a parabolic function (see the text).

represented by the power law, then the emission becomes optically thin and it is represented by the parabolic function with the maximum occurring at a frequency ν_{peak} . More complex and physically based models have been considered by others (e.g. Padovani et al 2003). But, as in our case the aim is to compare the peak frequencies amongst objects, it is sufficient to use a convenient analytical function for the modelling. The same protocol was used for all the objects. The flux densities were k-corrected, assuming the spectral indices from Sambruna et al. (1996) and in the computation of the luminosities a redshift of 0.3 was assumed³ if there was no redshift available for the object. When it was clear that the near infrared/optical emission was predominantly starlight (not AGN emission), the data points were ignored during the fitting process. We note that the optical data point is our estimate of the non-thermal emission,

³ We assume 0.3 because, for lower redshifts, it is often possible to resolve the host galaxy emission from the nuclear emission and measure the redshift of the former.

based on the 4000 Å break contrast as described in A04. Figure 1 shows the SEDs of four objects, each representing a different optical class: 1055+567 is a BL Lac, 0651+428 is a BL Lac Candidate, 0125+487 is a Seyfert-1 like object with blazar characteristics and 1241+735 is a PEG.

3 PEAK FREQUENCY & OPTICAL CLASSIFICATION

The SEDs were analysed in the manner described in the previous section and the distribution of the synchrotron peak frequencies (ν_{peak}) is shown in Figure 2. We draw attention to the fact that the ν_{peak} are widely and fairly *continuously* distributed from $\sim 10^{12}$ to 10^{16} Hz with the well-known BL Lacs ($C < 0.25$ & $EW < 5 \text{ \AA}$) and other objects ($C > 0.25$ & $EW > 5 \text{ \AA}$) occupying overlapping regions. The ν_{peak} distribution strongly points to the conclusion that we are dealing with a single group of objects drawn from the same population (otherwise one would not expect a continuous

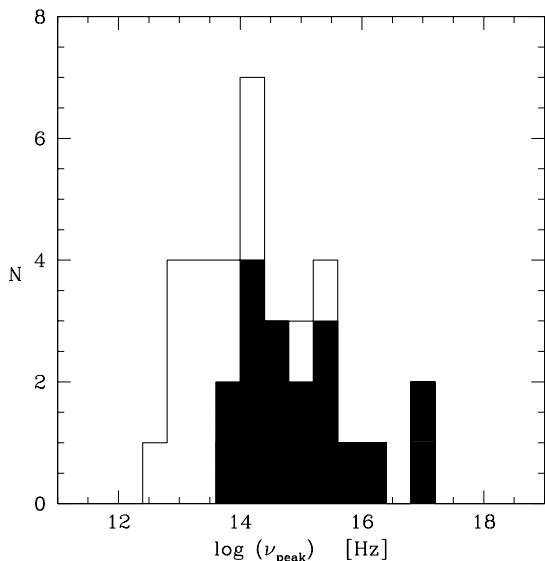


Figure 2. Peak frequency distribution of the objects in Table 1. Black area represent the ν_{peak} distribution of known BL Lac objects

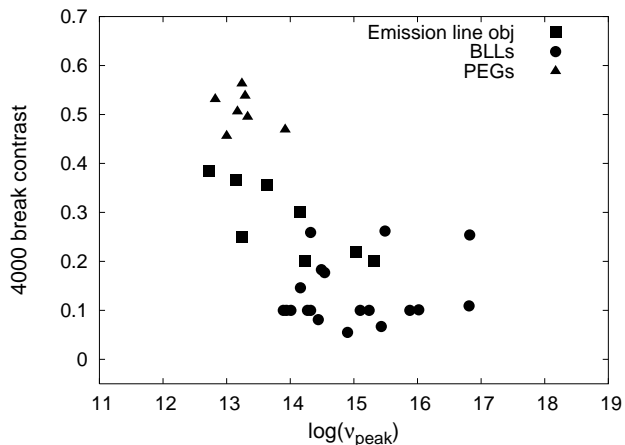


Figure 3. 4000 Å break contrast against peak frequency. The PEGs are represented by square symbols, Sey-like objects are represented by stars, BL Lac Candidate objects by triangles and BL Lac objects are represented by circles.

distribution), containing a wide spread of non-thermal cut-offs, ranging over 4 orders of magnitude in frequency.

In the lower frequency tail of the distribution, we suggest that we are seeing the red end of the blazar sequence and, if one wished to maintain the tradition of labelling objects by where their spectral peaks lie, one might call the objects with ν_{peak} lying at frequencies smaller than the near-infrared as Very Low-frequency-peaked BL Lacs, or VLBLs. We do not, however, believe it helpful to make this distinction and wish, rather, to emphasise the similarities. These objects:

- all have flat broad-band spectra up to frequencies of ~ 100 GHz or higher.
- all have radio structures that consist of compact VLBI cores plus jets.

How do the values of ν_{peak} relate to the traditional optical

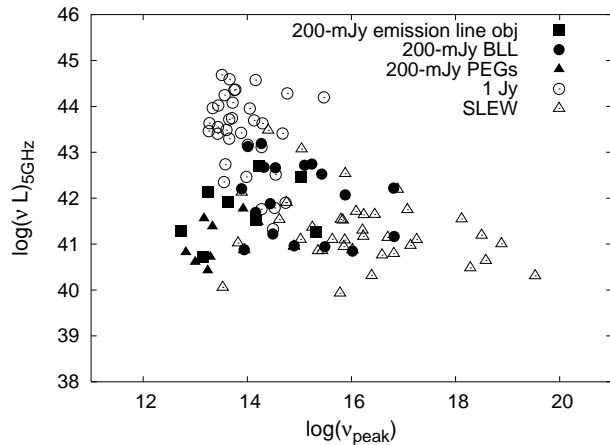


Figure 4. 5 GHz radio luminosity vs peak frequency for 1 Jy, Slew and 200 mJy objects. The latter are plotted in different symbols depending on whether they are known BL Lacs (BLLs), have emission lines or weak emission lines (PEGs)

classifications of BL Lacs, Seyfert-like objects and PEGs? It is of course of interest that not all the objects listed in Table 1, and that we would like to label as blazars, meet the usual “BL Lac” criteria. In Figure 3 the values of ν_{peak} are plotted against the 4000 Å break contrasts. As expected, the ν_{peak} distributions of BL Lacs are different from those of Seyfert-like, BL Lac Candidates and PEG objects; BL Lacs have ν_{peak} in the near-infrared/optical/X-ray bands and the rest of objects have their ν_{peak} located mainly between the long and near infrared bands. Of course it should be no surprise that the strength of the synchrotron component in the optical band (which is the basis of normal BL Lac classification) is dependent on the frequency at which the synchrotron emission begins to decline. Note that the importance of this effect on traditional classifications decreases with increasing non-thermal luminosity. In the case of powerful objects, their non-thermal optical component is strong enough to compete with the starlight (from the host galaxy) and to fill the 4000 Å break, even in the case of a relatively low ν_{peak} . That is, when there is a wide range of peak frequencies, as we believe is the case, it can lead to a selection-induced anti-correlation between ν_{peak} and luminosity (see below). This implies that a very low luminosity BL Lac is only recognised as such if it has a very high frequency peak, whereas for a high luminosity object recognition is possible for a wide range of peak frequencies.

4 THE TREND OF PEAK FREQUENCY WITH RADIO LUMINOSITY

A crucial question is whether or not the systematic shift of the average synchrotron peak frequency with luminosity, pointed out by Fossati et al. (1998) and Donato et al. (2001) is confirmed for our 200 mJy sample of low-luminosity radio-selected objects. This spectral sequence is important because, if true, it represents a great empirical simplification which is backed by an elegant physical explanation in terms of different inverse Compton losses occurring in the jet due to ambient photon densities which vary with object luminosity (Ghisellini et al. 1998; Georganopoulos et al.,

2001).

Unfortunately there are also selection effects which might give rise to a spurious correlation of the form that is observed (see also Perlman et al. 2001). This is because the result is based on all available blazar SEDs taken from a whole range of samples with different selection criteria. One of the possible selection effects – i.e. that recognition of BL Lacs with low cut of frequencies is more difficult at low luminosities than high luminosities – was already pointed out in Section 3. Another possible selection effect is that in the samples analysed by Fossati et al., the lower luminosity objects are mainly represented by the X-ray selected objects (e.g. the Slew sample) and therefore likely to be mainly HBL-type. On the other hand, the higher luminosity objects represented by the 1 Jy and 2 Jy samples, are mainly radio-selected objects, and therefore the majority are of LBL-type. Thus a correlation of the form observed could arise from the type of objects available for analysis.

The 200 mJy being a radio-selected sample, but of relatively low average radio-luminosity, occupies a critical range of parameter space and is thus well suited to enable us to check the reality of the radio-luminosity/spectral sequence: if they follow the expected luminosity trend, they should have high peak frequencies. To ensure that we are comparing like with like, the SEDs of the Slew and 1 Jy objects listed in Fossati et al (1998) were re-fitted in an identical manner to the 200 mJy objects (Section 2.2). Figure 4 presents the peak frequencies against radio luminosities at 5 GHz for the 1 Jy, Slew and 200 mJy objects (the latter plotted in different symbols depending on the optical classification). The 200 mJy objects fill a region of intermediate radio luminosity relative to the 1 Jy and Slew objects, showing objects with low radio luminosities and low peak frequencies. This is best shown in Figure 5 that presents the peak frequency distributions of the objects and their respective radio luminosities at 5 GHz. It is clear that the distributions of *radio luminosities* in the Slew survey and the 200 mJy samples are very similar. Thus, on the basis of the proposed spectral sequence, we would expect the 200 mJy objects and Slew objects to have the same distribution of *peak frequencies*. It is, however, evident from Figure 5 that they do not (K-S test rejects this hypothesis at a significance level of 2.4×10^{-5}). The 200 mJy peak frequency distribution is more similar to that of the 1 Jy sample, suggesting that the method of selection (i.e. radio or X-ray) has more influence on the peak frequency distribution than does the intrinsic luminosity.

We suggest that when there is a population with a broad distribution of spectral shapes, a low frequency band of selection biases the samples to objects that are stronger at low frequencies and a high frequency band of selection biases the samples to objects that are strong at high frequencies. Sources strong at low frequencies tend to have low peak frequencies and visa versa. In radio astronomical parlance, selecting at high frequencies is the way to select flat spectrum sources and selecting at low frequencies produces lots of steep spectrum sources (Kellermann et al., 1968). Also, as argued in Section 3, there is a bias against

recognising as traditional BL Lacs, low luminosity objects with synchrotron peak frequencies in the infrared and lower frequencies, which also acts to reinforce the Fossati et al. correlation.

5 DISCUSSION AND CONCLUSIONS

How valid is our approach to defining blazar samples? The advantage of ignoring the optical emission is that it is much less subject than other methods to luminosity-dependent selection effects, something that is quite important when comparing the statistical properties of samples with a range of luminosities.

Perhaps the most controversial thing we have done is to include objects with Seyfert-like spectra in our 200 mJy sub-sample. We point out, however, that three of the eight Seyfert-like objects, namely 0125+487, 1646+466 and 2116+81, are well-established blazars (Jackson & Marchã, 1999; Perlman et al., 1998). If we exclude the remaining five objects (see Figure 6) it is still clear that the peak frequency distribution for the 200 mJy sample objects is still much more like that of the 1Jy sample of high luminosity objects than that of the lower luminosity Slew survey objects (K-S test rejects the hypothesis that 200 mJy and Slew samples have similar peak frequency distributions at a significance level of 1.3×10^{-4}).

We thus believe that we have shown that amongst low-luminosity radio sources there are nuclear synchrotron emitters with peaks in their SEDs falling at lower frequencies than have been found before. These objects may not meet the criteria usually required for classification as a blazar but we see no good physical reason why they should be denied that status and argue that our “non-optical” method of sample selection has significant advantages over the tradition methods. Based on the assumption that these are really blazars, we have looked at where these objects fit on the sequence of blazar SEDs with luminosity investigated by Fossati et al. (1998) and Ghisellini et al. (1998). We find that they occupy part of the luminosity/peak frequency plane hitherto almost empty and thus much weaken the significance of the correlation found by Fossati et al. (1998) and Ghisellini et al. (1998). Our results are consistent with the results from Padovani et al. (2003). We compare peak frequency distributions of samples selected in diverse ways and argue that the distribution of peak frequencies for each sample has much more to do with the initial sample selection frequency than it has to do with intrinsic AGN luminosity.

6 ACKNOWLEDGMENTS

We thank Alessandro Caccianiga and Maria Marchã for useful discussions, and Eric Perlman for helpful comments. Sónia Antón acknowledges the financial support from the Portuguese Fundação para a Ciência e Tecnologia through the grant SFRH/BPD/5692/2001, the European Commission, TMR Programme, Research Network Contract ERBFMRXCT96-0034 “CERES” and the financial support from Jodrell Bank Observatory visitor grant. Ian Browne acknowledges the financial support from the Portuguese

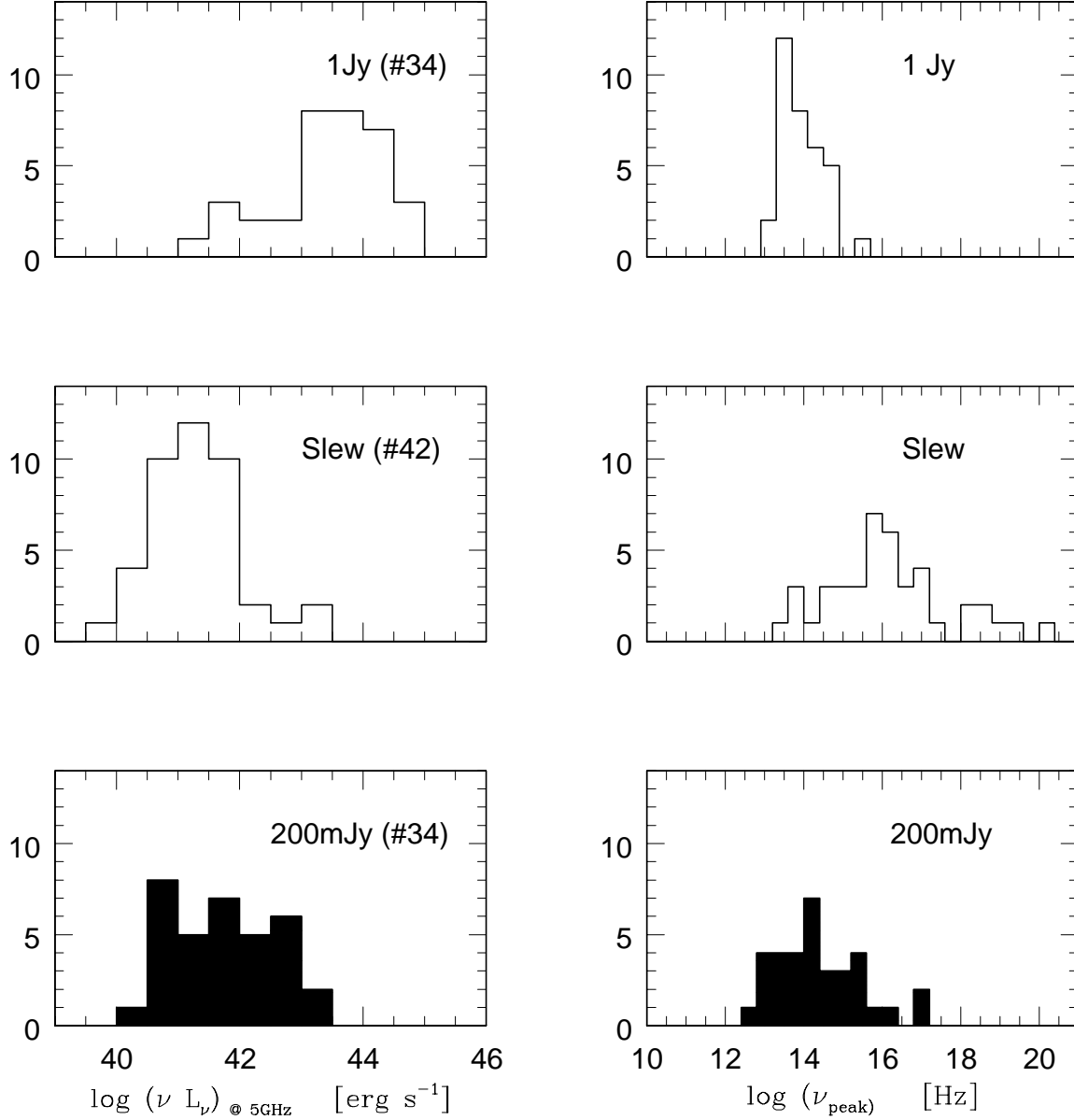


Figure 5. For each sample, 1 Jy (top), Slew (middle) and 200 mJy (bottom), the histograms on the left are the 5 GHz radio luminosity distribution and on the right the peak frequency distribution.

Fundação para a Ciência e Tecnologia through the project ESO/FNU/43803/2001.

REFERENCES

- Antón, S., Browne, I.W.A., Marchã, M.J.M., Bondi, M. & Polatidis, A., 2004, MNRAS, 352, 673.
 Augusto, P., Wilkinson, P. N. & Browne, I. W. A., 1998, MNRAS, 299, 1159.
 Blandford R. D. & Rees, M.J., 1978, in Pittsburgh Conference on BL Lac Objects, p. 328, Proceedings. (A79-30026 11-90) Pittsburgh, Pa., University of Pittsburgh
 Bondi, M., Marchã, M. J. M., Dallacasa, D., & Stanghellini, C. 2001, MNRAS, 325, 1109.
 Bondi, M., Marchã, M. J. M., Polatidis, A., Dallacasa, D., Stanghellini, C. & Antón, S., 2004, MNRAS, in press
 Browne, I. W. A & Marchã, M. J. M. 1993, MNRAS, 261, 795.
 Caccianiga, A., Marchã, M. J. M., Thean, A., & Dennett-Thorpe, J., 2001, MNRAS, 328, 867
 Caccianiga, A., Maccararo, T., Wolter, A., della Ceca, R.

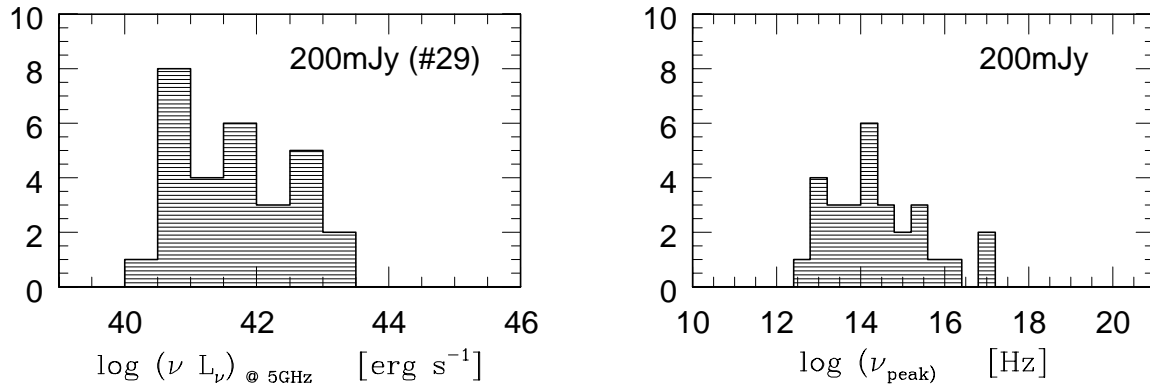


Figure 6. The histogram on the left is the 5 GHz radio luminosity distribution and on the right the peak frequency distribution of the objects listed in Table 1 except the following: 0251+393, 0309+411, 0321+340, 1421+511, 1744+260

- & Gioia, I. M., 1999, *ApJ*, 513, 51
- Donato, D., Ghisellini, G., Tagliaferri, G., & Fossati, G. 2001, *A&A*, 375, 739
- Fossati, G., Celotti, A., Ghisellini, G., & Maraschi, L. 1997, *MNRAS*, 289, 136
- Fossati, G., Maraschi, L., Celotti, A., Comastri, A. & Ghisellini, G., 1998, *MNRAS*, 299, 433
- Gabuzda, D. C., Cawthorne, T. V., Roberts, D. H. & Wardle, J. F. C. 1989, *ApJ*, 347, 701.
- Gabuzda, D. C., Sitko, M. L. & Smith, P. S., 1996, *AJ*, 112, 1877.
- Gabuzda, D. C. & Cawthorne, T. V., 1996, *MNRAS*, 283, 759.
- Gabuzda, D. C., Kovalev, Y. Y., Krichbaum, T. P., Alef, W., Kraus, A., Witzel, A. & Quirrenbach, A., 1998, *A&A*, 333, 445.
- Georganopoulos, M., Kirk, J. G., & Mastichiadis, A. 2001, *ASP Conf. Ser. 227: Blazar Demographics and Physics*, 116. Edited by Paolo Padovani and C. Megan Urry.
- Ghisellini, G., Celotti, A., Fossati, G., Maraschi, L. & Comastri, A., 1998, *MNRAS*, 301, 451
- Ghisellini, G., Celotti, A., & Costamante, L. 2002, *A&A*, 386, 833
- Gioia, I. M., Maccacaro, T., Schild, R. E., Wolter, A., Stocke, J. T., Morris, S. L. & Henry, J. P., 1990, *ApJS*, 72, 567
- Henstock, D. R., Browne, I. W. A., Wilkinson, P. N., Taylor, G. B., Vermeulen, R. C., Pearson, T. J. & Readhead, A. C. S., 1995, *ApJS*, 100, 1
- Jackson, N. & Marchã, M. 1999, *MNRAS*, 309, 153
- Kellermann, K. I., Pauliny-Toth, I. I. K. & Davis, M. M. 1968, *Astrophysical Letters*, 2, 105
- Kellermann, K. I., Vermeulen, R. C., Zensus, J. A. & Cohen, M. H., 1998, *AJ*, 115, 1295.
- Kollgaard, R. I., 1994, *Vistas in Astronomy*, 38, 29
- Kollgaard, R. I., Gabuzda, D. C. & Feigelson, E. D., 1996, *ApJ*, 460, 174.
- Landt, H., Padovani, P. & Giommi, P., 2002, *MNRAS*, 336, 945.
- Landt, H., Padovani, P., Perlman, E. S. & Giommi, P. 2004, *MNRAS*, 351, 83.
- Laurent-Muehleisen, S. A., Kollgaard, R. I., Ciardullo, R., Feigelson, E. D., Brinkmann, W. & Siebert, J., 1998, *ApJS*, 118, 127
- Maccacaro, T., Wolter, A., McLean, B., Gioia, I. M., Stocke, J. T., della Ceca, R., Burg, R. & Faccini, R., 1994, *ApL&C*, 29, 267
- Marchã & Browne, 1995, *MNRAS*, 275, 951
- Marchã, M. J. M., Browne, I. W. A., Impey, C. D. & Smith, P. S. 1996, *MNRAS*, 281, 425
- Padovani, P., Perlman, E. S., Landt, H., Giommi, P., & Perri, M. 2003, *ApJ*, 588, 128
- Pearson, T. J., Readhead, A. C. S., Barthel, P. D., Conway, J. E. & Myers, S. T., 1993, *AAS*, 25, 869.
- Perlman, E. S., Padovani, P. Giommi, P., Sambruna, R., Jones, L. R., Tzioumis, A. & Reynolds, J., 1998, *AJ*, 115, 1253
- Perlman, E. S., Padovani, P., Landt, H., Stocke, J. T., Costamante, L., Rector, T., Giommi, P. & Schachter, J. F. 2001, *ASP Conf. Ser. 227: Blazar Demographics and Physics*, 200. Edited by Paolo Padovani and C. Megan Urry.
- Piner, B. G., Unwin, S. C. Wehrle, A. E., Edwards, P. G., Fey, A. L. & Kingham, K. A., 1999, *ApJ*, 525, 176.
- Polatidis, A. 1989, *MSc. thesis*, University of Manchester.
- Rector, T. A., Stocke, J. T., Perlman, E. S., Morris, S. L. & Gioia, I. M., 2000, *AJ*, 120, 1626
- Rector, T. A. & Stocke, J. T. 2001, *AJ*, 122, 565
- Sambruna, R. M., Maraschi, L. & Urry, C. M., 1996, *ApJ*, 463, 444
- Stickel, M., Fried, J. W., Kuhr, H., Padovani, P. & Urry, C. M. 1991, *ApJ*, 374, 431
- Stocke, J. T., Morris, S. L., Gioia, I. M., Maccacaro, T., Schild, R., Wolter, A., Fleming, T. A. & Henry, J. P. 1991, *ApJS*, 76, 813
- Taylor, G. B., Vermeulen, R. C., Pearson, T. J., Readhead, A. C. S., Henstock, D. R., Browne, I. W. A., & Wilkinson, P. N. 1994, *ApJS*, 95, 345
- Taylor, G. B., Vermeulen, R. C., Readhead, A. C. S., Pearson, T. J., Henstock, D. R. & Wilkinson, P. N., 1996, *ApJS*, 107, 37.
- Urry, C. M. & Padovani, P., 1995, *PASP*, 107, 803

Venturi, T., Giovannini, G., Feretti, L., Comoreto, G. &
Wehrle, A. E., 1993, ApJ, 408, 81.